Journal of Power Sources 293 (2015) 823–830

Contents lists available at ScienceDirect

Journal of Power Sources

journal homepage: www.elsevier.com/locate/jpowsour

Binary and ternary palladium based electrocatalysts for alkaline direct glycerol fuel cell

Adriana Napoleão Geraldes [a], Dionisio Furtunato da Silva [b], Leonardo Gondim de Andrade e Silva [b], Estevam Vitório Spinacé [b], Almir Oliveira Neto [b], Mauro Coelho dos Santos [a, *]

[a] Laboratório de Eletroquímica e Materiais Nanoestruturados, Centro de Ciências Naturais e Humanas, Universidade Federal do ABC, Rua Santa Adélia, 166, 09210-170, Santo André-SP, Brazil
[b] Instituto de Pesquisas Energéticas e Nucleares-Comissão Nacional de Energia Nuclear (IPEN-CNEN), Av. Prof. Lineu Prestes, 2242, 05508-900, São Paulo-SP, Brazil

HIGHLIGHTS

- Palladium based electrocatalysts.
- Electron beam irradiation reduction process.
- Single alkaline direct glycerol fuel cell.
- PdAuSn/C 50:40:10 electrocatalyst show the higher power density.

ARTICLE INFO

Article history:
Received 3 April 2015
Received in revised form
18 May 2015
Accepted 2 June 2015
Available online 11 June 2015

Keywords:
Alkaline direct glycerol fuel cell
Palladium-based
Durability tests
Electron beam irradiation
Glycerol electro-oxidation

ABSTRACT

Pd/C, PdAu/C 50:50, PdSn/C 50:50, PdAuSn/C 50:40:10 and PdAuSn/C 50:10:40 electrocatalysts are prepared using an electron beam irradiation reduction method and tested for glycerol electro-oxidation in alkaline medium. X-Ray diffraction (XRD), Energy dispersive X-ray analysis (EDX), Transmission electron Microscopy (TEM) and Cyclic Voltammetry (CV) are used to characterize the resulting materials. The activity for glycerol electro-oxidation is tested in alkaline medium at room temperature using Cyclic Voltammetry and Chronoamperometry (CA) and in a single alkaline direct glycerol fuel cell (ADGFC) at temperature range of 60–90 °C. EDX analysis demonstrate that Pd:Au:Sn atomic ratios are very similar to the nominal ones. X-ray diffractograms of PdAuSn/C electrocatalysts evidence the presence of Pd (fcc), Au (fcc) and SnO_2 phases. TEM analysis demonstrates a good dispersion of the nanoparticles on the carbon support with some agglomerates. Cyclic Voltammetry experiments suggest that PdAuSn/C electrocatalysts demonstrate better results. In single fuel cell tests, at 85 °C, using 2.0 mol L^{-1} glycerol in 2.0 mol L^{-1} KOH solutions, the electrocatalyst PdAuSn/C 50:40:10 demonstrate highest power density (51 mW cm^{-2}) and the 120 h durability tests demonstrate a 210 μV h^{-1} degradation rate.

© 2015 Elsevier B.V. All rights reserved.

1. Introduction

In the current situation, where world's energy system needs to be changed radically in the next decades, researches on materials, processes and systems are provided as a critical aspect for the development of a clean and more efficient energy system. The environmental problems and the global demand for energy have stimulated the scientific community to research clean and renewable energy sources [1–3].

Due to their high energy efficiency, convenient operation, and friendly environmental characteristics, polymer electrolyte membrane fuel cells (PEMFC) are considered one of the most promising fuel cell technologies for both stationary and mobile applications. Significant progress has been achieved over the past few decades. However, durability and cost have been identified as the most important issues in PEMFC technology. Durability is one of the major difficults to have polymer electrolyte membrane fuel cells

* Corresponding author.
E-mail addresses: drinager@ig.com.br (A.N. Geraldes), dfsilva@ipen.br (D.F. da Silva), lgasilva@ipen.br (L.G.A. e Silva), espinace@ipen.br (E.V. Spinacé), aolivei@ipen.br (A.O. Neto), pdrmcsa@gmail.com (M.C. dos Santos).

http://dx.doi.org/10.1016/j.jpowsour.2015.06.010
0378-7753/© 2015 Elsevier B.V. All rights reserved.

(PEMFC), accepted as a viable commercial product. Electrocatalyst degradation mechanisms depend on factors such as potential, temperature, humidity, contaminants, and carbon support stability [4].

In this context, fuel cells appear to be an appropriate technology for generating electricity through the electro-oxidation of alcohols [5–9].

When compared to hydrogen-fed fuel cells the direct alcohol fuel cell, (DAFC) is more interesting because the use of liquid fuels simplifies the fuel delivery system [5,6,10–12]. Primary alcohols such as ethanol, 1-propanol, ethylene glycol, and glycerol have demonstrated to be interesting as fuels in DAFC for several reasons, such as, their low toxicity, high boiling point, high specific energy and less prominent crossover due to their larger molecular size [13].

Recently, the electro-oxidation of glycerol in fuel cells to add value to the large amount of this alcohol - generated as a byproduct of biodiesel used as fuel in internal combustion engines of fleets of large cities - have been studied. The glycerol electro-oxidation could bring environmental benefits and economic feasibility to biodiesel production. Although the complete electro-oxidation of glycerol to CO_2, is hard due to the need of C–C bond breaking. The use of glycerol - a non-valued residue of biodiesel production - as fuel may be an interesting alternative, because it is less toxic than methanol and displays relatively lower theoretical energy density, 5.0 kWh kg^{-1}, *versus* 6.1 kWh kg^{-1} for methanol [14]. Alkaline medium should be preferred to acid medium since the electrochemical reaction kinetics occurring at fuel cell electrodes - fuel oxidation [15] and oxygen reduction [15,16] – are favored and lower platinum loadings or platinum-free electrocatalysts could be used [17].

It has been reported that palladium is an active metal for glycerol and/or ethanol electro-oxidation [14,18–21]. On the other hand, gold is generally considered as a poor electrocatalyst in acid medium; however, its activity in alkaline medium is slightly greater. The reactivity of glycerol and ethanol on gold, in alkaline medium, is related to the fact that, practically, no poisoning species (CO-like species) may be formed and adsorbed on the surface [22], however tin is also studied in the literature.

Pd/C and PdSn/C were studied by Liu et al. [23] as catalysts for formic acid oxidation. PdSn/C has higher electrocatalytic activity for formic acid electro-oxidation than a comparative Pd/C catalyst and it shows great potential as a less expensive electrocatalyst for formic acid electro-oxidation in direct formic acid fuel cells (DFAFC). Du et al. [24] studied a series of carbon-supported Pd–Sn binary alloyed catalysts, as anode electrocatalysts, for direct ethanol fuel cell reactions in an alkaline medium. Among various Pd–Sn catalysts, $Pd_{86}Sn_{14}$/C catalysts showed a great deal of enhanced current densities in cyclic voltammetric and chronoamperometric measurements, compared to commercial Pd/C (Johnson Matthey). The overall rate law of ethanol oxidation reaction, for both $Pd_{86}Sn_{14}$/C and commercial Pd/C, was also determined, showing that $Pd_{86}Sn_{14}$/C was more favorable in high ethanol concentration and/or high pH environment.

The nature, structure, and composition of multi-metallic catalysts have an important effect on the alcohol electro-oxidation in terms of activity (energy generation) and selectivity. Considering that the chemical and physical characteristics of these electrocatalysts depend on the preparation procedure, this becomes a key factor regarding their electrochemical activity [12]. In our studies, the carbon-supported metal nanoparticles have been prepared for fuel cell applications using radiation-induced reduction of precursors of metal ions [25]. Silva et al. prepared PtRu/C electrocatalysts for methanol electro-oxidation, in acid medium, using gamma irradiation and electron beam irradiation [26–28]. Silva et al. [25] also prepared $PtSnO_2$/C electrocatalysts for ethanol electro-oxidation, in acid medium, using electron beam irradiation. Moreover, Silva et al. [28] studied the activity of the electrocatalysts for alcohol oxidation in alkaline medium and the results showed that PtAu/C electrocatalysts had a better performance for methanol electro-oxidation when compared to other electrocatalysts prepared. PtAuBi/C (50:40:10) indicated a superior performance for ethanol electro-oxidation in alkaline medium [28]. Geraldes et al. [29,30] prepared carbon-supported Pd, Au and bimetallic PdAu (Pd:Au 90:10, 50:50 and 30:70 atomic ratios) electrocatalysts using electron beam irradiation for ethanol and glycerol electro-oxidation. In ethanol electro-oxidation [29], chronoamperometry (CA) experiments, at room temperature, demonstrated that PdAu/C electrocatalysts with Pd:Au ratios of 90:10 and 50:50, presented superior activity. Using *in-situ* ATR-FTIR spectroscopy measurements it was observed that the mechanism for ethanol electro-oxidation is dependent on catalyst composition, leading to different reaction products such as acetaldehyde and acetate, depending on the number of electrons transferred. Experiments on a single alkaline direct ethanol fuel cell (ADEFC) were conducted between 50 and 90 °C, and the best performance of 44 mW cm^{-2} in 2.0 mol L^{-1} ethanol was obtained at 85 °C for Pd:Au with Pd:Au atomic ratio 90:10 electrocatalyst. Geraldes et al. [30] also studied the glycerol electro-oxidation in single alkaline direct glycerol fuel cell (ADGFC). Cyclic voltammetry (CV) and chronoamperometry showed that PdAu/C electrocatalyst with Pd:Au atomic ratio of 50:50 indicated superior activity for glycerol electro-oxidation at room temperature. Using *in-situ* ATR-FTIR spectroscopy experiments it was identified oxalate, glycerate oxalate, glycerate ion, 1,3-dihydroxy-2-propanone, glyceraldehyde and glycolate as products of glycerol electro-oxidation. Experiments with single ADGFC were carried out from 50 to 90 °C, using Pd/C electrocatalyst: the best performance was obtained at 80 °C. In another study [31], Pd and PdSn (Pd:Sn atomic ratios of 90:10), supported on Multi Wall Carbon Nanotubes (MWCNT) or Carbon (C), were prepared. CV analysis finds that Pd/MWCNT and PdSn/MWCNT present onset potentials changing to negative values and high current values, compared to Pd/C and PdSn/C electrocatalysts. In-situ ATR-FTIR analysis identified acetate and acetaldehyde as principal products formed during the ethanol electro-oxidation with low conversion to CO_2. In single fuel cell tests, at 85 °C, using 2.0 mol L^{-1} ethanol in 2.0 mol L^{-1} KOH solutions, the electrocatalysts supported on MWCNT, showed higher power densities, compared to the materials supported on carbon: PdSn/MWCNT presented the best result (36 mW cm^{-2}). The results demonstrated that the use of MWCNT improves the electrocatalytic activity for Ethanol Oxidation Reaction (EOR).

In our laboratory, we have prepared electrocatalysts for electron beam irradiation reduction process [25–31]. Considering that binary PdAu/C and PdSn/C electrocatalysts prepared according to this methodology showed good activity for glycerol and ethanol electro-oxidation in alkaline medium [28–31], we proposed a study of ternary electrocatalysts. In this regard, the aim of this paper is focused on the preparation of ternary PdAuSn/C electrocatalysts and test of these materials for glycerol electro-oxidation in an alkaline medium at room temperature using electrochemical techniques and in a single ADGFC at 60–90 °C.

2. Experimental

Pd/C, PdAuSn/C50:40:10, PdAuSn/C 50:10:40, PdAu/C 50:50 and PdSn/C 50:50 electrocatalysts (20 wt% metal loading), were prepared using $Pd(NO_3)_2.2H_2O$ (Fluka), $HAuCl_4$ $3H_2O$ (Fluka), and $SnCl_2$ (Fluka) as metal sources, dissolved in 50/50 (v/v) water/2-propanol. Carbon Vulcan® XC72R used as a support, was, then, dispersed in the solution using an ultrasonic bath. The resulting mixtures were

submitted (at ambient conditions) to stirring under electron beam irradiation (Electron Accelerator's Dynamitron Job 188–IPEN/CNEN–SP), with a total applied dose of 288 kGy (dose rate 1.6 kGy s^{-1}, time 3 min). After electron beam irradiation, the mixtures were filtered and the solids (Pd/C, PdAuSn/C, PdAu/CPdSn/C electrocatalysts) were washed with water and dried at 70 °C for 2 h, according to a previous work [29–31].

Pd:Au:Sn, Pd:Au and Pd:Sn atomic ratios were obtained by energy-dispersive X-ray analysis (EDX), using a Philips XL30 scanning electron microscope, with a 20 keV electron beam and equipped with an EDAX DX-4 microanalyzer.

X-ray diffraction (XRD) analysis were carried out with a Miniflex II, model Rigaku diffractometer, using a Cu Kα source (λ = 1.54056 Å). The diffractograms were recorded at 2θ in the range 20–90°, with step size of 0.05° and scan time of 2s per step. The average crystallite size was estimated using the Debye-Scherrer's equation [32].

Transmission electron microscopy (TEM) was carried out using a JEOL JEM-2100 electron microscope, operated at 200 kV. The particle distribution histogram was determined by measuring about 150 particles from each micrograph.

Electrochemical studies were carried out using the thin porous coating technique [33]. A total of 20 mg of the electrocatalyst was added to a solution of 50 mL of water containing 3 drops of a 6% polytetrafluoroethylene (PTFE) suspension. The resulting mixture was treated in an ultrasound bath for 10 min, filtered and transferred to the cavity (0.30 mm deep and 0.36 cm^2 in area) of the working electrode. The reference electrode was Ag/AgCl (KCl 3 mol L^{-1}) homemade electrode, and the counter electrode was a Pt plate.

Electrochemical measurements were carried out using an AutoLab PGSTAT 30 potentiostat/galvanostat. Cyclic voltammetry was performed using 1.0 mol L^{-1} glycerol in 1.0 mol L^{-1} KOH, saturated with N_2. Chronoamperometry experiments were performed using 1.0 mol L^{-1}glycerol in 1.0 mol L^{-1} KOH at −0.30 V vs. Ag/AgCl, (KCl 3 mol L^{-1}), at room temperature.

Membrane electrode assemblies (MEA) were prepared by hot pressing a Fumasep-FAA3-PEEK membrane (Fumasep FAA3 reinforced with PEEK and pre-treated in 1.0 mol L^{-1} KOH, for 24 h) between an anode of Pd, PdAu, PdSn or PdAuSn supported by C (prepared in this study), and a cathode of 20 wt% Pd/C, at 80 °C for 2 min under pressure of 45 kgf cm^{-2}. Both electrodes used 1.0 mg metal cm^{-2} catalyst loading. The ink, containing 70 wt % catalysts + support and 30 wt % Nafion, was painted in carbon cloth. The MEA was placed between two bipolar plates and assembled in a single fuel cell with a 6 Nm torque wrench. The experiments were performed using a test bench from Electrocell Group that allows control over the fuel cell operating parameters (flow rates, humidification and temperature of the reactants and cell temperature), performing automatic data acquisition of polarization curves and power density curves, in real time. A Masterflex L/S Cole–Parmer peristaltic pump was used for liquid fuel alimentation. The direct glycerol fuel cell performances were determined in a single cell with a geometric area of 5 cm^2. The temperature was set between 60 and 90 °C, for the fuel cell, and 85 °C for the oxygen humidifier. The 2.0 mol L^{-1} glycerol fuel in 2.0 mol L^{-1} KOH was delivered at 1.0 mL min^{-1}, and the oxygen flow was regulated at 500 mL min^{-1}. Polarization curves were obtained by using a CDE electronic load. In the durability test 100 mA was set at, and the initial potential was 530 mV and the variation voltage was measured over the operation time.

3. Results and discussion

The atomic ratios obtained by using EDX for PdAuSn/C 50:40:10, PdAuSn/C 50:10:40, PdAu/C 50:50 and PdSn/C 50:50 electrocatalysts are summarized in Table 1.

Table 1
Nominal Pd:Au:Sn, Pd:Au and Pd:Sn atomic ratios, those obtained by EDX.

Pd:Au:Sn atomic ratio (nominal)	Pd:Au:Sn atomic ratio (EDX)
PdAuSn/C 50:40:10	36:56:08
PdAuSn/C 50:10:40	45:19:36
PdAu/C 50:50	58:42
PdSn/C 50:50	46:54

For ternary electrocatalysts the atomic ratios determined by using EDX analysis demonstrated higher content of gold when compared to the nominal ones. For samples, Pd:Au and Pd:Sn the atomic ratios were similar to the nominal ones, indicating that most of the metal ions contained in the mixtures were reduced to metal and chemically anchored to the support [29–31].

The XRD diffractograms of Pd/C, PdAuSn/C 50:40:10, PdAuSn/C 50:10:40, PdAu/C 50:50 and PdSn/C 50:50 electrocatalysts were displayed in Fig. 1.

The X-ray diffractograms displayed in Fig. 1 showed a broad peak centered at about 2θ = 25° (Bragg angle) that was attributed to reflection plane (002) of the hexagonal structure of Carbon Vulcan XC-72R (C) support. The four diffraction peaks related to the Pd are showed at 2θ, approximately, 40°, 46°, 68° and 82°, associated with the reflection planes (111), (200), (220) and (311), respectively, which are characteristic of the face-centered cubic (fcc) structure of Pd [22,26,34,35]. Five peaks related to Au were observed at about 2θ = 38°, 45°, 65°, 78° and 82°, attributed to the (111), (200), (220), (311) and (222) planes, respectively, which are characteristic of the fcc structure of Au [36]. In the diffractograms the position of the peaks of Pt(fcc) and Au(fcc) are not shifted indicating no alloy formation between them. For PdAuSn/C electrocatalyst it could be also observed two peaks at about 2θ = 38° and 52° that were attributed to a SnO_2 phase [25,37–39]. Our previous study of PtSn/C electrocatalysts prepared by electron beam irradiation reduction [25], showed that Pt exists as Pt(fcc) phase and Sn as an SnO_2 phase, which was identified using ^{119}Sn Mössbauer spectroscopy. Based on these results, we could infer that Pd(fcc), Au(fcc) and a SnO_2 phase coexist on PdAuSn/C electrocatalysts.

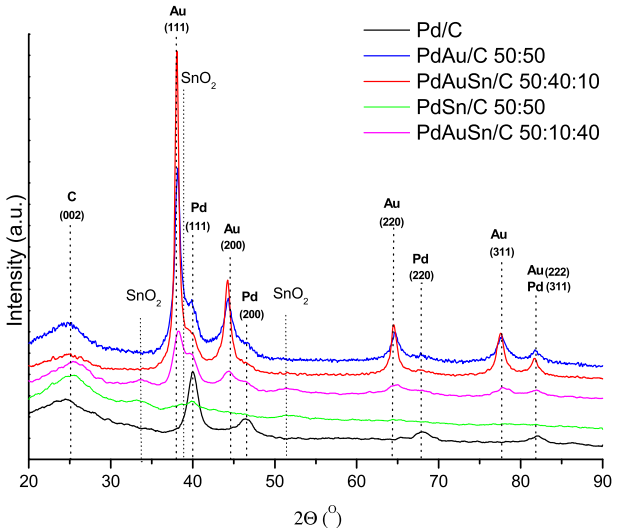


Fig. 1. X-ray diffractograms of Pd/C, PdAuSn/C 50:40:10, PdAuSn/C 50:10:40, PdAu/C 50:50 and PdSn/C 50:50 electrocatalysts.

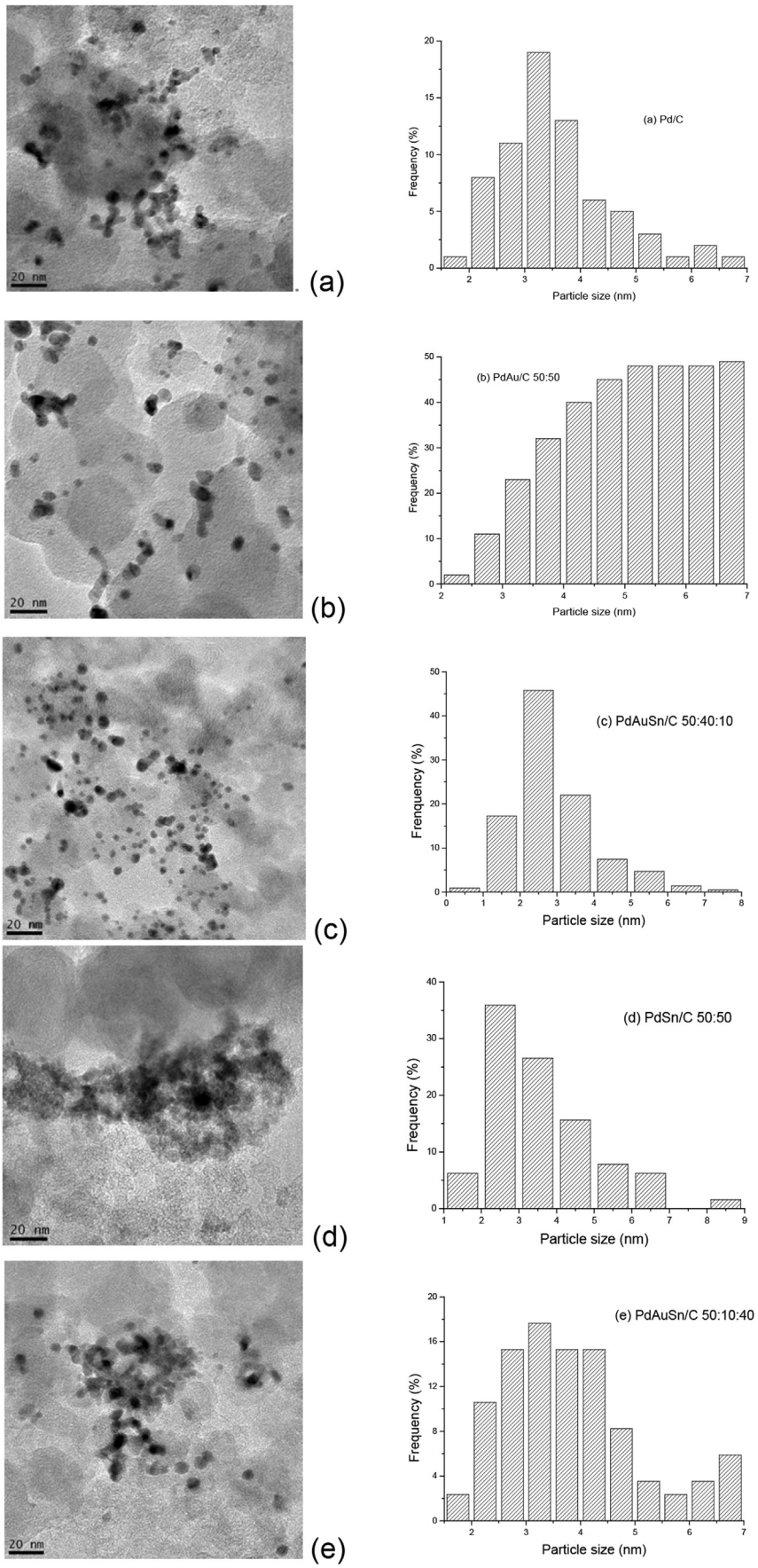


Fig. 2. TEM micrographs and particle size distribution histograms of (a) Pd/C, (b) PdAu/C (50:50), (c) PdAuSn/C (50:40:10), (d) PdSn/C (50:50) and (e) PdAuSn/C (50:10:40) electrocatalysts.

TEM micrographs of electrocatalysts studied showed morphology, particle size, and their distribution histograms (Fig. 2).

The TEM micrographs of Pd/C, PdAu/C and PdAuSn/C (Pd:Au atomic ratio 50:50 and Pd:Au:Sn atomic ratio 50:40:10) electrocatalysts showed a good distribution of nanoparticles on the carbon support with an average particle size between 3 and 7 nm. The PdSn/C 50:50 and PdAuSn/C 50:10:40 electrocatalysts showed some agglomeration of the nanoparticles on the carbon support with particle sizes in the range of 2–7 nm.

The voltammetric responses for glycerol oxidation using Pd/C, PdAu/C (50:50), PdAuSn/C (50:40:10), PdSn/C (50:50) and PdAuSn/C (50:10:40) electrocatalysts are shown in Fig. 3.

The cyclic voltammogram obtained from glycerol electro-oxidation on Pd/C electrocatalyst showed the highest onset potential: −0.65 V *vs.* Ag/AgCl. The onset potential from glycerol oxidation for PdAu/C (50:50), PdAuSn/C (50:40:10), PdSn/C (50:50) and PdAuSn/C (50:10:40) electrocatalysts were −0.59, −0.60, −0.61 and −0.60 V *vs.* Ag/AgCl), respectively. These results showed that the addition of Au and/or Sn to Pd/C electrocatalyst provides a beneficial effect on the performance in the whole potential range. The best performance of the binary or ternary electrocatalysts may be attributed to the bifunctional mechanism where Pd species are available for glycerol adsorption and Au and/or Sn provide oxygen species for the oxidation of the intermediates [30].

Fig. 4 showed the chronoamperometry obtained at room temperature in solutions 1.0 mol L^{-1} KOH in 1.0 mol L^{-1} glycerol at a fixed potential of −0.30 V *vs.* Ag/AgCl, for 30 min, concerning the Pd/C, PdAu/C (50:50), PdAuSn/C (50:40:10), PdSn/C (50:50) and PdAuSn/C (50:10:40) electrocatalysts.

The electrocatalysts prepared were tested for 30 min to evaluate the electrocatalysts activity, stability and tolerance to poisoning by intermediate species. In all experiments, the current density reaches a stable condition and the electrocatalyst stability can be evaluated. The peaks that occur in the first few seconds are due to charging double layer and the instability of the system under the conditions in which the experiment was performed. After this short interval the system stabilized. For all the electrodes, the measurement demonstrated a slight fall in the current value for the studied electrocatalysts, probably associated with no restoration of fuel or poisoning of the electrode, due to the formation and adsorption of intermediate species generated during the glycerol electro-oxidation, in the time interval measured. From the graphs, it was observed that the electrocatalyst Pd/C presented a more

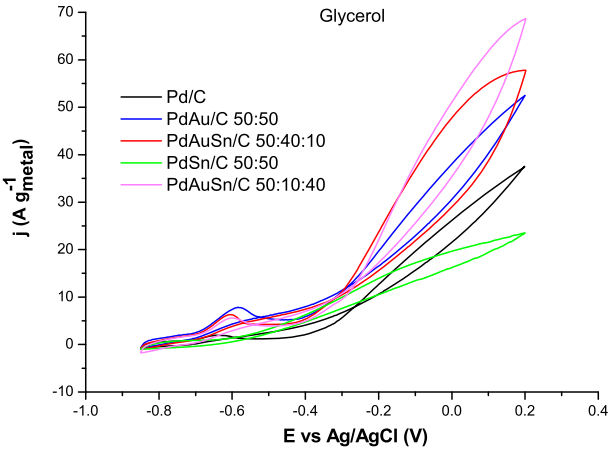


Fig. 3. Cyclic voltammograms of Pd/C, PdAu/C (50:50), PdAuSn/C (50:40:10), PdSn/C (50:50) and PdAuSn/C (50:10:40) electrocatalysts in 1.0 mol L^{-1} glycerol and 1.0 mol L^{-1} KOH, measured over potential range from −0.85 to +0.20 V *vs.* Ag/AgCl, at sweep rate of 10 mV s^{-1}.

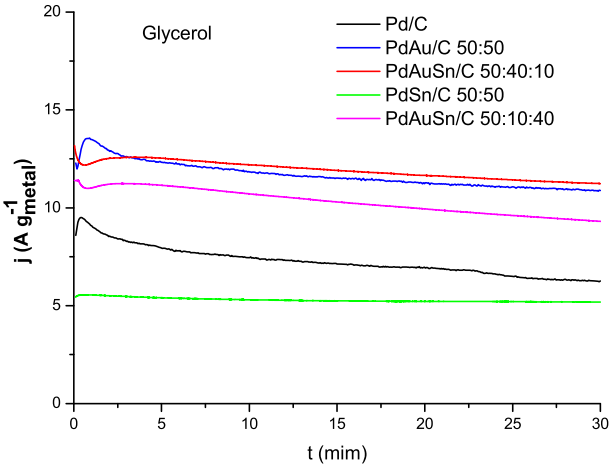


Fig. 4. Current-time curves at −0.40 V for Pd/C, PdAu/C (50:50), PdAuSn/C (50:40:10), PdSn/C (50:50) and PdAuSn/C (50:10:40) electrocatalysts, in 1.0 mol L^{-1} glycerol in 1.0 mol L^{-1} KOH.

pronounced drop in the density current value, while the electrocatalysts PdAu/C (50:50), PdAuSn/C (50:40:10), PdSn/C (50:50) and PdAuSn/C (50:10:40) were more stable, since the decrease in the current density was less substantial. It was also observed that the electrocatalysts PdAu/C (50:50), PdAuSn/C (50:40:10) were the most active among all the evaluated ones and PdSn/C (50:50) electrocatalyst provided an oxidation current lower than the pure Pd/C. These results suggest that in the investigated electrode potential, the addition of Au and/or Sn at electrocatalyst Pd/C contributes to the activity and stability of Pd-based electrocatalysts, toward glycerol electro-oxidation, yielding more efficient and tolerant to poisoning electrocatalysts. This fact may be attributed to the synergistic effect that gold and/or tin carries on palladium and to bifunctional mechanism.

The single fuel cells performance at the temperature range 60–90 °C of Pd/C, PdAu/C (50:50), PdAuSn/C (50:40:10), PdSn/C (50:50) and PdAuSn/C (50:10:40) electrocatalysts, fed with 1.0 mL min^{-1} solution 2.0 mol L^{-1} glycerol in 2.0 mol L^{-1} KOH, at room temperature are shown in Fig. 5.

The performance of each electrode was significantly improved as the temperature increased, indicating that the glycerol electro-oxidation processes are thermally activated. The highest current and power densities were obtained at approximately 85 °C indicating that this is the best operating temperature of MEAs based on palladium. Above this temperature, water management and membrane dryness began to interfere with electrode performance, most likely due to an increase in cell resistance [29–31].

These results indicate that a better reactant diffusion and higher kinetics of the electrodes may be achieved at higher temperatures. Problems were not detected with fuel diffusion in the electrodes since, in the polarization curves, a maximum current was reached without exponential decay associated to the mass transport limitations, i. e. the curves do not exhibit accentuated decay in the concentration over potential region. The increase of power density, increasing the fuel cell temperature, also, suggests that the membrane used in MEA has low permeability to glycerol, since an increase in the cell operating temperature favors the ions mobility in the membrane, raising the fuel permeability toward the cathode. This fact would promote the occurrence of parallel reactions between the fuel and OH^- species, present in the cathode, creating a potential mix and reducing the cell overall potential. Nevertheless, this phenomenon was not observed in the graph [40].

The main results from the single ADGFC experiments are summarized in Table 2.

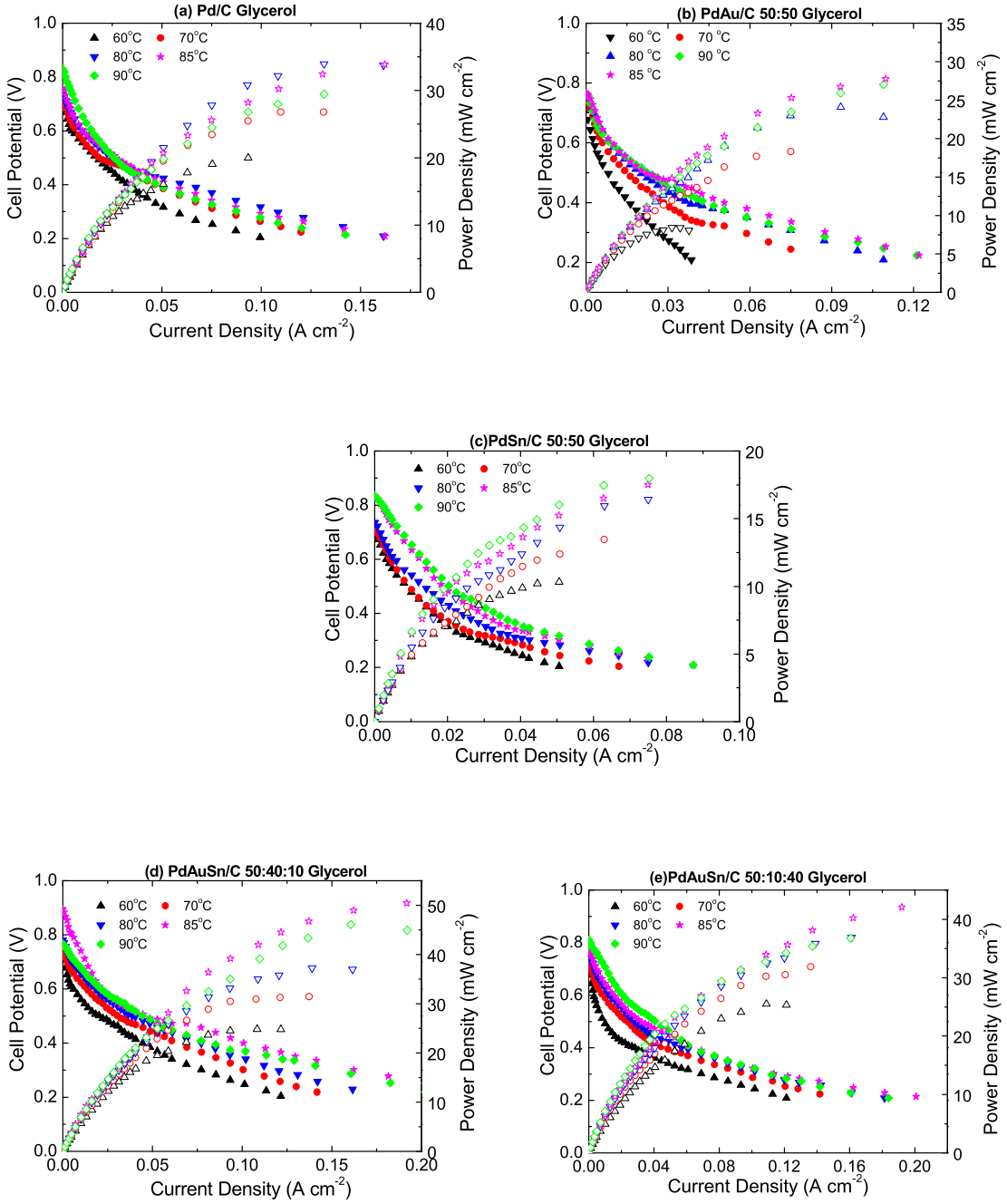


Fig. 5. Polarization and power density curves of a 5 cm^2 ADGFC, using a Fumasep-FAA-PEEK membrane, operating from 60 to 90 °C and using a (a) Pd/C, (b) PdAu/C (50:50), (c) PdSn/C (50:50), (d) PdAuSn/C (50:40:10) and (e) PdAuSn/C (50:10:40)anodic electrocatalyst and a Pd/C cathodic electrocatalyst fed with 2.0 mol L^{-1} glycerol in 2.0 mol L^{-1} KOH solution; the anodic and cathodic catalyst loading levels were both 1 mg cm^{-2} and oxygen humidifier at 85 °C.

Table 2
Values of maximum power density achieved in the temperature range 60–90 °C of Pd/C, PdAu/C (50:50), PdAuSn/C (50:40:10), PdSn/C (50:50) and PdAuSn/C (50:10:40) electrocatalysts, fed with 1.0 mL min^{-1} solution 2.0 mol L^{-1} glycerol in 2.0 mol L^{-1} KOH, and oxygen flow of 500 mL min^{-1} (both at atmospheric pressure).

	P_{max}/mWcm^{-2}				
T/°C	Pd/C	PdAu/C 50:50	PdSn/C 50:50	PdAuSn/C 50:40:10	PdAuSn/C 50:10:40
60	20	8	10	25	25
70	27	18	13	31	32
80	32	24	16	37	37
85	34	28	17	51	42
90	29	27	18	46	37

In Table 2, comparing the Pd/C electrocatalyst to binary electrocatalysts (PdAu/C and PdSn/C), it was observed that the adding gold or tin to the catalyst did not improve the power density. The power density of the PdSn/C electrocatalyst (17 mW cm^{-2}) was half of Pd/C (34 mW cm^{-2}) electrocatalyst.

The values in Table 2 showed that the highest power density generated at 85 °C was 51 mW cm^{-2}, obtained with the PdAuSn/C 50:40:10 MEA, followed by 42 mW cm^{-2} with the PdAuSn/C 50:10:40 MEA.

Glycerol electro-oxidation by PdAuSn/C 50:40:10 electrocatalyst produces 17 mW cm^{-2} more than Pd/C, while the PdAuSn/C 50:10:40 produces 8 mW cm^{-2}, generating 50 and 20% higher power density respectively, when compared to Pd/C. These data suggest that both co-catalysts (Au and Sn) are important to catalytic activity and that, to a higher current density, a larger amount of Pd sites is necessary. The current increase was significant and may be associated with the presence of gold and tin oxides, which increases the amount of oxides and increase the available amount of Pd active sites and (b) due to a better distribution of nanoparticles in support probably due to the preparation method. The single-cell tests showed that the addition of Au and Sn to Pd enhances the activity of ternary electrocatalyst (Fig. 6).

Zhang et al. [41] studied carbon supported Pt, Pd, and Au nanoparticles prepared through a solution-phase reduction method and applied as the model catalysts for electro-oxidation of both high-purity glycerol and biodiesel-derived crude glycerol. The anion-exchange membrane fuel cells (AEMFCs) investigations demonstrated no obvious drop in peak power density on Pt/C anode, when the fuel was changed from high-purity glycerol to crude glycerol, indicating a good stability of the Pt/C against poisoning/deactivation from the impurities in crude glycerol. The highest performances were achieved with 6.0 mol L^{-1} KOH +1.0 mol L^{-1} crude glycerol at 80 °C, which are 184.2, 93.9, and 50.1 mW cm^{-2} on Pt/C, Pd/C, and Au/C anodes, respectively.

Mougenot et al. [42] studied PdAu (70:30) catalyst, alternate sputtered PdAuPd (35:30:35) and AuPdAu (15:70:15) materials prepared by using plasma deposition of Au and Pd atoms, on a carbon diffusion layer. The modification of palladium surface by gold atoms leads to an increase in the catalytic activity toward glycerol electro-oxidation. The PdAu surface alloy composition has no significant effect on the catalytic activity; however, the presence of non-alloyed gold sites on the material surface leads to the enhancement of the catalytic activity. The mechanism seems to involve glycerol adsorption on palladium surface and hydroxyl species formation on gold surface, leading to catalytic activity enhancement through the bifunctional mechanism. Lie et al. [19] tested a commercial anionic membrane FUMAPEM® FAA from Fumatech. The tests were performed in a 5 cm^2 cell with identical anode and cathode (Pt (40 wt%)/C, 2 mgPt cm^{-2} deposited on a diffusion layer carbon cloth with PTFE (15 wt%)/C. The used fuel composition was glycerol 1.0 mol L^{-1}/NaOH 4.0 mol L^{-1}, and oxygen was used as oxidant. The power densities achieved with the Fumatech membrane was 13.5 mW cm^{-2}, at 60 °C and 7.8 mW cm^{-2}, at 25 °C.

The values in Fig. 6 provided two major observations: (i) the power densities were higher in the ternary electrocatalysts; (ii) the addition of only one co-catalyst to Pd/C is not efficient for glycerol electro-oxidation. In previous research, Geraldes et al. [30] studied binary electrocatalysts (PdAu in different atomic ratios) for glycerol oxidation reaction and observed that the large amount of gold as co-catalyst is not efficient (50 or 70 parts of Au). The highest power densities were 34, 33, 29 and 25 mW cm^{-2}, obtained with Pd/C, PdAu/C 90:10, PdAu/C 50:50 and PdAu/C30:70 MEAs, respectively.

The durability test was applied to the MEA, which provided higher power density (51 mWcm^{-2}), namely, Pd/C (catode)–Fumasep-FAA-3 PEEK (electrolyte)–PdAuSn/C 50:40:10 (anode), fed with 1.0 mL min^{-1} solution 2.0 mol L^{-1} glycerol in 2.0 mol L^{-1} KOH. In the durability test the current was set at 100 mA, the initial

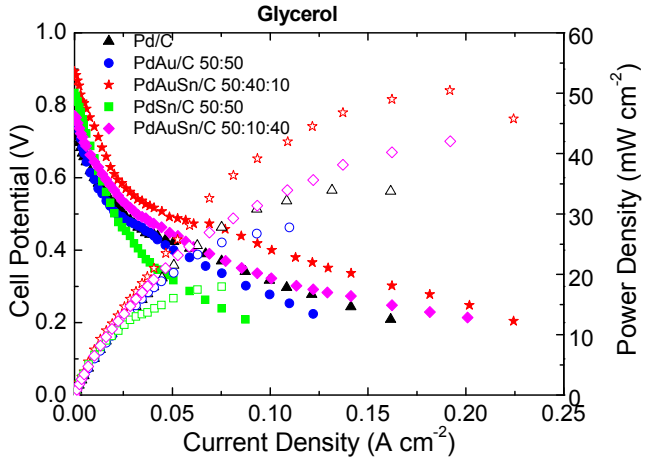


Fig. 6. Polarization and power density curves of a 5 cm^2 ADGFC, using a Fumasep-FAA-PEEK membrane, operating from 85 °C and using a Pd/C, PdAu/C (50:50), PdSn/C (50:50), PdAuSn/C (50:40:10) and PdAuSn/C (50:10:40) anodic electrocatalyst and a Pd/C cathodic electrocatalyst fed with 2.0 mol L^{-1} ethanol in 2.0 mol L^{-1} KOH solution; the anodic and cathodic catalyst loading levels were both 1 mg cm^{-2} and oxygen humidifier at 85 °C.

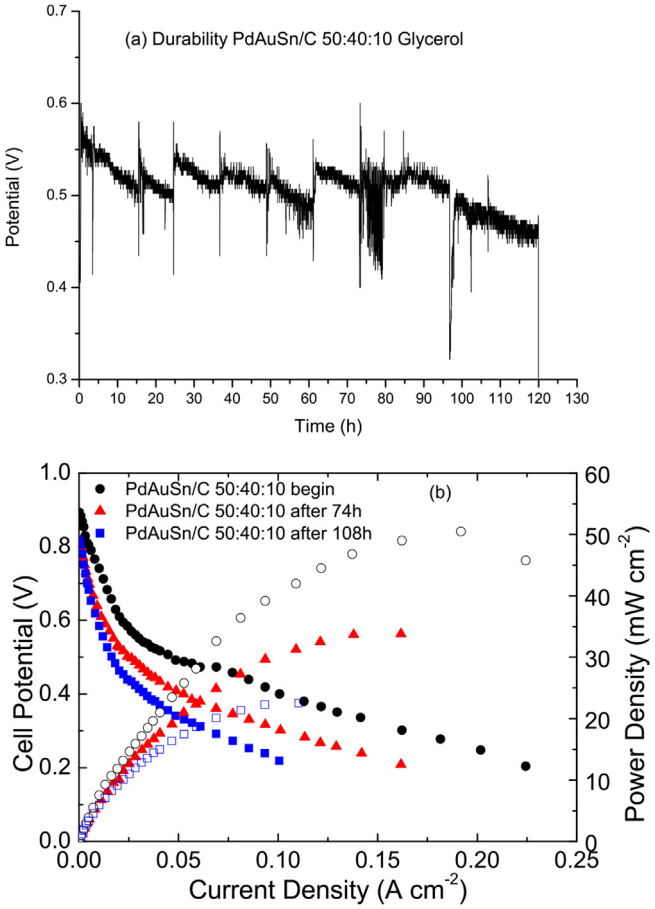


Fig. 7. Potential-time curves (a), obtained every 5 s, using MEA Pd/C (catode)–Fumasep-FAA-3 PEEK (electrolyte)–PdAuSn/C 50:40:10 (anode), fed with 2.0 mol L^{-1} glycerol in 2.0 mol L^{-1} KOH solution; the anodic and cathodic catalyst loading levels were both 1 mg cm^{-2} and oxygen humidifier at 85 °C. The cell was at 85 °C. Polarization and power density curves (b) of a 5 cm^2 ADGFC initial, after 74 h and 108 h.

potential was 530 mV and the variation voltage was measured over the operation time. During the operation time, periodic shutdowns occurred at night. The interval between the stops was approximately 10 h and the duration of each operating period was approximately 12 h. From the data obtained it was possible to estimate the potential variation rate of the cell during the operation time, considering the steady state operation.

The durability curves (potential-time) with periodic stops, and polarization and power density curves before and after the durability tests for the MEA Pd/C (catode)- Fumasep-FAA-3 PEEK (electrolyte)-PdAuSn/C 50:40:10 (anode) are shown in Fig. 7.

The graph in Fig. 7a showed several series points with potential decays due to periodic stops that occurred during the experiment. This fact can be attributed to the imbalance of operating conditions such as temperature, oxygen humidification, flooding or drying of the electrodes. that need to be defined for long-term testing. The MEA Pd/C (catode)– Fumasep-FAA-3 PEEK (electrolyte)–PdAuSn/C 50:40:10 (anode) can be operated for about 120 h. After this time, the experiment cuts off and cannot be restarted. The maximum power densities in Fig. 7b were 51, 34 and 22 mW cm^{-2} in the begining, 74 and 108 h respectively and the losses in the efficiency of the fuel cell system were 67% (74 h) and 43% (108 h). The degradation rate of this MEA was at 210 μV h^{-1}. This degradation rate is not comparable to the literature. Usually, degradation targets require less than 20% loss in the efficiency of the fuel cell system by the end of its life, and a degradation rate of 2–10 μV h^{-1} is commonly accepted for most applications [4,43]. Various failure modes have been identified such as preferential alloy dissolution in the catalyst layer, carbon support oxidation (corrosion), and catalyst poisoning [4]. However, such speculations were not the subject of these studies. Although the degradation rate is still higher than the literature reports, this preliminary durability tests show a good starting for assessing the electrocatalysts with better performance in fuel cell.

4. Conclusions

The addition of only Au or only Sn to Pd-electrocatalysts does not change their activities significantly for glycerol electrooxidation in alkaline medium; however, when they are added together the activity could be improved. Among the electrocatalysts tested, PdAuSn/C with Pd:Au:Sn atomic ratio of 50:40:10 showed superior activity. In single direct alkaline glycerol fuel cell, the best performance was obtained at 85 °C and above this temperature the fuel cell performance becames unstable and fell. The maximum power density obtained was 51 mW cm^{-2} and durability tests of 120 h showed a degradation rate of 210 μV h^{-1}. The promoting effect of Au and Sn could be explained by a bifunctional mechanism, where Au and Sn would adsorb and increase the concentration of OH^- species, on proximity to Pd, favoring the oxidation of glycerol/intermediary adsorbed in the Pd surface. This results demonstrate the possibility of replacing part of palladium for gold or tin electrochemical performance without loss of electrochemical performance. It can be inferred that the co-catalysts (Au and Sn) of Pd based electrode materials contribute to a dissociative oxidation of glycerol.

Acknowledgments

The authors wish to thank FAPESP, CNPq (162669/2013-5, 474913/2012-0, 406612/2013-7), INCT Instituto Nacional de Ciência e Tecnologia (INCT) Energia e Meio Ambiente (Process Number: 573.783/2008-0) and CTR and CCTM from IPEN/CNEN-SP for electron beam irradiations and TEM measurements.

References

[1] F. Barbir, PEM Fuel Cells, Academic Press, Theobald's Road, London, 2013.
[2] M. Carmo, G. Doubek, R.C. Sekol, M. Linardi, A.D. Taylor, J. Power Sources 230 (2013) 165–169.
[3] A. Brouzgou, S.Q. Song, P. Tsiakaras, Appl. Catal. B: Environ. 127 (2012) 371–388.
[4] X.Z. Yuan, H. Li, S. Zhang, J. Martin, H. Wang, J. Power Sources 196 (2011) 9107–9116.
[5] S.Y. Shen, T.S. Zhao, J.B. Xu, Y.S. Li, J. Power Sources 195 (2010) 1001–1006.
[6] A.O. Neto, R.R. Dias, M.M. Tusi, M. Linardi, E.V. Spinacé, J. Power Sources 166 (2007) 87–91.
[7] H. Liu, C. Song, L. Zhang, J. Zhang, H. Wang, D.P. Wilkinson, J. Power Sources 155 (2006) 95–110.
[8] A. Brouzgou, A. Podias, P. Tsiakaras, J. Appl. Electrochem. 43 (2013) 119–136.
[9] L.V. Kumar, S.A. Ntim, O.S. Khow, C. Janardhana, V. Lakshminarayanan, S. Mitra, Electrochimica Acta 83 (2012) 40–46.
[10] W.J. Zhou, W.Z. Li, S.Q. Song, Z.H. Zhou, L.H. Jiang, G.Q. Sun, Q. Xin, K. Poulianitis, S. Kontou, P. Tsiakaras, J. Power Sources 131 (2004) 217–223.
[11] S. Rousseau, C. Coutanceau, C. Lamy, J.M. Léger, J. Power Sources 158 (2006) 18–24.
[12] E. Antolini, J. Power Sources 170 (2007) 1–12.
[13] F.E. Teran, D.M. Santos, J. Ribeiro, K.B. Kokoh, Thin Solid Films 520 (2012) 5846–5850.
[14] M. Simões, S. Baranton, C. Coutanceau, Appl. Catal. B: Environ. 93 (2010) 354–362.
[15] C.C. Yang, Int. J. Hydrog. Energy 29 (2004) 135–143.
[16] Y. Wang, L. Li, L. Hu, L. Zhuang, J. Lu, B. Xu, Electrochem. Commun. 5 (2003) 662–666.
[17] L. Demarconnay, C. Coutanceau, J.M. Leger, Electrochimica Acta 49 (2004) 4513–4521.
[18] M. Simões, S. Baranton, C. Coutanceau, Appl. Catal. B: Environ. 110 (2011) 40–49.
[19] A. Ilie, M. Simões, S. Baranton, C. Coutanceau, S. Martemianov, J. Power Sources 196 (2011) 4965–4971.
[20] C. Xu, R. Zeng, P.K. Shen, Z. Wei, Electrochimica Acta 51 (2005) 1031–1035.
[21] V. Bambagioni, C. Bianchini, A. Marchionni, J. Fillipi, F. Vizza, J. Teddy, P. Serp, M. Zhiani, J. Power Sources 190 (2009) 241–251.
[22] G. Tremiliosi-Filho, E.R. Gonzalez, A.J. Motheo, E.M. Belgsir, J.M. Léger, C. Lamy, J. Electroanal. Chem. 444 (1998) 31–39.
[23] Z. Liu, X. Zhang, Electrochem. Commun. 11 (2009) 1667–1670.
[24] W. Du, K.E. Mackenzie, D.F. Milano, N.A. Deskins, D. Su, X. Teng, ACS Catal. 2 (2012) 287–297.
[25] D.F. Silva, A.N. Geraldes, A.O. Neto, E.S. Pino, M. Linardi, E.V. Spinacé, W.A.A. Macedo, J.D. Ardisson, Material Sci. Eng. B 175 (2010) 261–265.
[26] D.F. Silva, A.O. Neto, E.S. Pino, M. Linardi, E.V. Spinacé, J. Power Sources 170 (2007) 303–307.
[27] D.F. Silva, A.O. Neto, E.S. Pino, M. Brandalise, M. Linardi, E.V. Spinacé, Material Res. 10 (2007) 367–370.
[28] D.F. Silva, A.N. Geraldes, E.Z. Cardoso, M.M. Tusi, M. Linardi, E.V. Spinacé, A.O. Neto, Int. J. Electrochem. Sci. 6 (2011) 3594–3606.
[29] A.N. Geraldes, D.F. Silva, E.S. Pino, J.C.M. Silva, R.F.B. Souza, P. Hammer, E.V. Spinacé, A.O. Neto, M. Linardi, M.C. Santos, Electrochimica Acta 111 (2013) 455–465.
[30] A.N. Geraldes, D.F. Silva, J.C.M. Silva, R.F.B. Souza, E.V. Spinacé, A.O. Neto, M. Linardi, M.C. Santos, J. Braz. Chem. Soc. 25 (2014) 831–840.
[31] A.N. Geraldes, D.F. Silva, J.C.M. Silva, O.A. de Sá, E.V. Spinacé, A.O. Neto, M.C. Santos, J. Power Sources 245 (2014) 189–199.
[32] V. Radmilovic, H.A. Gasteiger, P.N. Ross, J. Catal. 154 (1995) 98–106.
[33] A.O. Neto, M.J. Giz, J. Perez, E.A. Ticianelli, E.R. Gonzalez, J. Electrochem. Soc. 149 (2002) A272–A279.
[34] J. Belloni, M. Mostafavi, H. Remita, J.L. Marignier, M.O. Delcourt, New J. Chem. 22 (1998) 1239–1255.
[35] S.L. Medway, C.A. Lucas, A. Kowal, R.J. Nichols, D. Johnson, J. Electroanal. Chem. 587 (2006) 172–181.
[36] A.F. Lee, C.J. Baddeley, C. Hardacre, R.M. Ormerod, R.M. Lambert, J. Phys. Chem. 99 (1995) 6096–6102.
[37] E. V. Spinacé, A. O. Neto, M. Linardi, D. F. Silva, E. S. Pino, V. A. Cruz, Patent BR200505416-A.
[38] E.V. Spinacé, M. Linardi, A.O. Neto, Electrochem. Commun. 7 (2005) 365–369.
[39] W.S. Cardoso, M.S.P. Francisco, A.M.S. Lucho, Y. Gushikem, Solid State Ionics 167 (2004) 165–173.
[40] Q.H. Zeng, Q.L. Liu, I. Broadwell, A.M. Zhu, Y. Xiong, X.P. Tu, J. Membr. Sci. 349 (2010) 237–243.
[41] Z. Zhang, L. Xin, J. Qi, D.J. Chadderdon, W. Li, Appl. Catal. B: Environ. 136–137 (2013) 29–39.
[42] M. Mougenot, A. Caillard, M. Simões, S. Baranton, C. Coutanceau, P. Brault, Appl. Catal. B: Environ. 107 (2011) 372–379.
[43] J. Wu, X.Z. Yuan, J.J. Martin, H. Wang, J. Zhang, J. Shen, J. Power Sources 184 (2008) 104–119.